Airtanker Flight Distance between Fires: Random Fire Starts on Line Segments

Francis E. Greulich

Abstract: Under high initial attack fire loads, dispatchers sometimes redirect airtankers that are working on other fires. The inherent variability of flight distance between random fire locations is a potentially important aspect of any model that would reallocate the airtanker resource between fires. Requisite formulas are derived, and computational procedures are provided in this article for the stochastic description of airtanker flight distances between fire-start locations randomly located along straight-line segments. Numerical approximations and comparisons with prior work confirm the results of detailed examples that establish a blueprint for application and continued model development. FOR. SCI. 51(5):460–471.

Key Words: Operations research, spatial statistics, transportation planning, travel distance.

ISLAM AND MARTELL (1998) indicate that amphibious land-based airtankers may be dispatched directly from one fire to another. Although acknowledging this observed fire-to-fire dispatch strategy, they assume, for modeling purposes, that airtanker dispatches only involve airtankers being sent directly from an airbase to a fire. In their investigation, Islam and Martell are interested in the response of the airtanker initial attack (ATIA) system to changes in the daily fire load. They found that the optimal initial attack range around an airbase depends on the daily fire load. However, it seems quite likely that, as the fire load increases, the proportion of direct fire-to-fire airtanker dispatches will also increase. Under these circumstances, it is expected that inclusion of a fire-to-fire dispatch option within airtanker system models may eventually lead to a more accurate portrayal of actual system behavior under high fire load conditions.

The fire-to-fire reallocation component of the ATIA model envisions reallocation of the airtanker from one randomly located fire to another fire, also randomly located. Anticipatory, model-based planning for dispatch of airtankers directly between ATIA fires requires a probabilistic assessment of their spatial distribution. The locations of two simultaneous ATIA fires can be described for mathematical modeling as point-events randomly located at points, along line segments, or over polygonal regions. A statistical description of the random flight distance between simultaneous initial attack fires should include all six possible pairings of points, line segments, and areas. For random travel distances between points, between a point and a line segment, or between a point and an area, there are well-established formulas and analytical procedures for first and second moments about the origin. Interested readers are referred to the article by Greulich (2003) for these formulas and a brief history of their development. Okabe and Miller (1996) give formulas for the expected distance in all six cases but they do not provide formulas for higher moments, nor are potential computational issues examined for the variety of intersecting and overlapping elements typically observed in airtanker applications.

Martell et al. (1999) identify airtanker travel time as a "very significant portion of the service time." Accordingly, the expected flight distances between airbase, fire location, and landable lakes are key parameters in the estimation of service times (Islam and Martell 1998). This fundamental relationship between service time and travel distance is not unique to airtanker system performance. For example, Larson and Odoni (1981) associate this characteristic with a wide range of spatially distributed public and private service activities. Larson and Odoni, analyzing primarily urban services, emphasize de novo analytic development of statistical parameters for rectilinear travel over geometrically simple regions. Airtanker systems, however, can be more accurately described, and efficiently analyzed, using programmable analytical procedures that use standard, closed-form equations and assume straight-line travel over geometrically complex regions (Greulich 2003). The use of closed-form equations in the analytical development of travel time parameters can bring definite advantages in computational flexibility, speed, and precision. The availability of these closed-form equations also opens up potential new lines of research. It is then the purpose of this article to continue previous development of these analytical procedures based on closed-form equations, mention some of their advantages, and illustrate their application to a simple, hypothetical problem.

As a first step in the development of an ATIA fire-to-fire reallocation component, this article examines the statistical description of the random distance between fires occurring along line segments. An example is used to illustrate a fire-protection setting within which the formulas and procedures, to be developed in this article, might be applicable.

Francis E. Greulich, Professor, College of Forest Resources, University of Washington, Seattle, WA 98195-2100—Phone: (206) 543-1464; Fax: (206) 685-3091; greulich@u.washington.edu.

Manuscript received September 8, 2003, accepted February 1, 2005

A discussion of some alternative ways in which the statistical problem might be addressed is followed by development of the requisite formulas and their verification. With formulas and associated analytical procedures in hand, the illustrative example is revisited and its solution developed. The article concludes with several observations on current research motivation and direction in the statistical description of fire-to-fire reallocation of airtankers.

Illustrative Problem Setting

Two components of a hypothetical ATIA region, a transportation corridor and a wildland–urban interface, are shown in Figure 1. These two components, each of considerable length, have been modeled as chains of linear elements because of their curving nature and relatively narrow widths. Their inclusion in the model is based on their having high ATIA fire probabilities relative to the surrounding area. For simplicity of exposition, the ATIA region will be assumed to consist of only these two components.

When a fire, classified as subject to possible ATIA, starts within one of these two strips, the dispatcher establishes its priority relative to other demands and the availability of suppression forces. It is possible, especially under high fire loads, that an airtanker already assigned and working on an initial attack fire will be redirected to the new fire-start location. There will be some delay in arriving at the new fire, and this elapsed time will vary depending, in part, on the distance separating the two fires.

ATIA planning relies on good estimates of flight-time delay in arriving at a fire. As a first pass at evaluating airtanker travel times between concurrent ATIA fires, the simple formula that time equals the distance divided by the airtanker cruise speed may be used. The general form of this equation is the same as that for the flight-time component of total service time in the article by Islam and Martell (1998). Also borrowing from Islam and Martell, it is assumed that the airtanker has a mean cruising speed of 250 km/hr. In the absence of additional information, this speed will be treated here as if it were a constant [1].

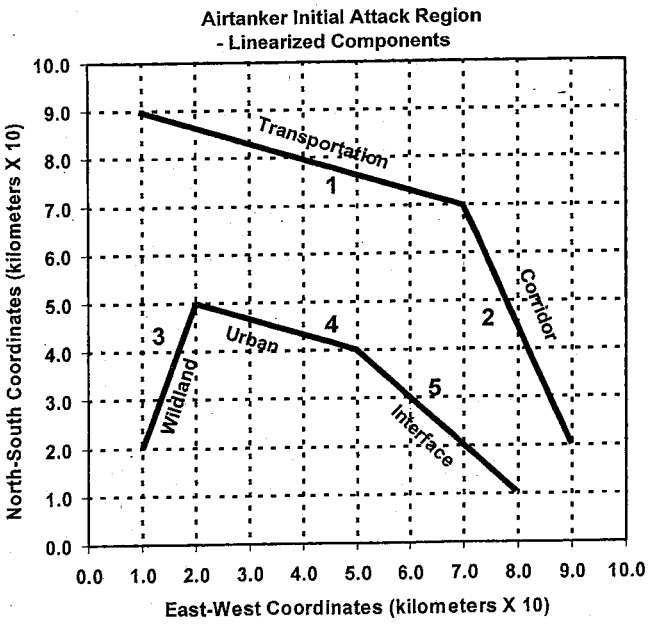

Figure 1. Hypothetical airtanker initial attack example illustrating application of the formulas and computational procedure.

For illustrative purposes, it is assumed that an ATIA fire will start at some random location along one of the five line segments shown in Figure 1. The probability of its occurrence on each of the five segments has been specified and its specific location on any given segment is assumed to follow a uniform distribution over the length of the segment [2]. The airtanker resource is dispatched to this first fire. While working at this fire, a second ATIA fire is reported. The location of this second fire follows the same probability distribution as the first. In modeling the ATIA system, it is desirable to know statistical characteristics of the flight distance between concurrent fires such as these. These descriptive measures would include the mean and variance of the flight distance. Based on these flight-distance parameters and the given airtanker cruising speed, an average flight time between concurrent fires may be calculated along with an estimate of its variability. Formulas and procedures leading to the calculation of these operational variables are now developed and verified before continuing with the example.

Solution Methodology

There are at least three ways in which the illustrative example of the previous section could be evaluated for the requisite flight-distance parameters: Monte Carlo simulation of the airtanker transfer process, numerical integration of the corresponding moment equations, and analytical integration. The latter method, analytical integration, will be used to provide closed-form equations for the statistical moments. All three methodologies have been successfully applied to this example, but for brevity of presentation, only the last two are reported here in detail.

Calculating the expected, or mean, distance between random points located on line segments requires two formulas, one for parallel line segments and a second for nonparallel segments. The latter formula, but not the former, is explicitly presented in Okabe and Miller (1996). In airtanker applications, it is also necessary that overlapping and crossing line segments be included as possible configurations. Formulas for higher moments (not developed by Okabe and Miller) are needed when calculating the expected value of a nonlinear cost or flight-time model. These higher moments may also be used in the calculation of model variability (Ang and Tang 1975). The necessity for recognizing and incorporating travel-time variability in models of the initial attack system has been dramatically shown in the simulation studies done by Smith (1987). Smith found this aspect of fire modeling to be of particular importance when examining simultaneous fires. He notes that serious resource misallocation can result from the use of averages where large variations in travel time are found. One additional recommendation for a new derivation of the moment formulas is found in the form of the equations. The

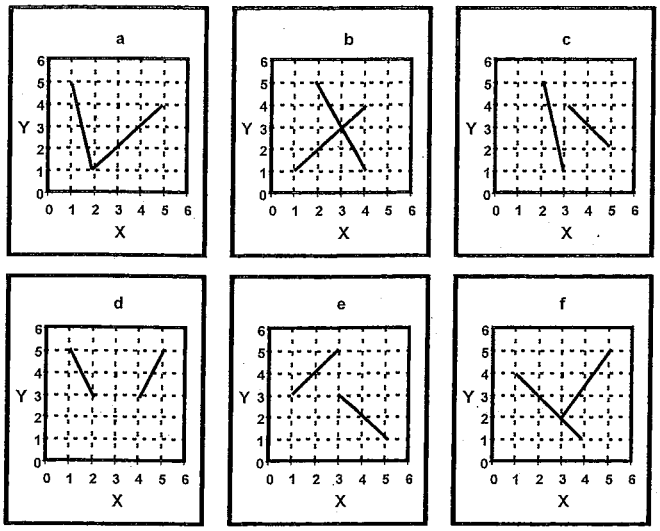

Figure 2. Specific examples of the six possible configurations of two nonparallel segments.

moment equation formulas are more compactly written and structurally revealing when recorded in terms of length and area rather than point coordinates, as listed in Okabe and Miller. This format is also consistent with previous usage in forestry, thereby facilitating derivation and application of the formulas in that field of study. A brief overview, including background relevant to the development of these crucial formulas, will follow. The more analytical aspects of formula derivation are covered in the appendixes.

The derivation of the formula for expected travel distance between two nonparallel line segments given in this article (Appendix A) follows a distinctly different development from that outlined by Okabe and Miller (1996). In this current derivation, the use of Crofton's formulation and previously published results for the expected travel distance from a point to a line substantially shorten the development. Derived in this alternative manner, the formula also provides an opportunity for mutual verification with the results presented by Okabe and Miller. The second moment of the flight-distance distribution is derived in a similar fashion. These two formulas are specific to a particular spatial configuration of the line segments, an example of which is

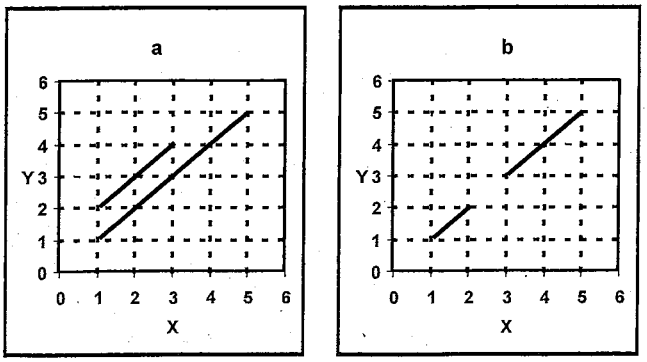

Figure 3. Specific examples of the two possible configurations of parallel segments.

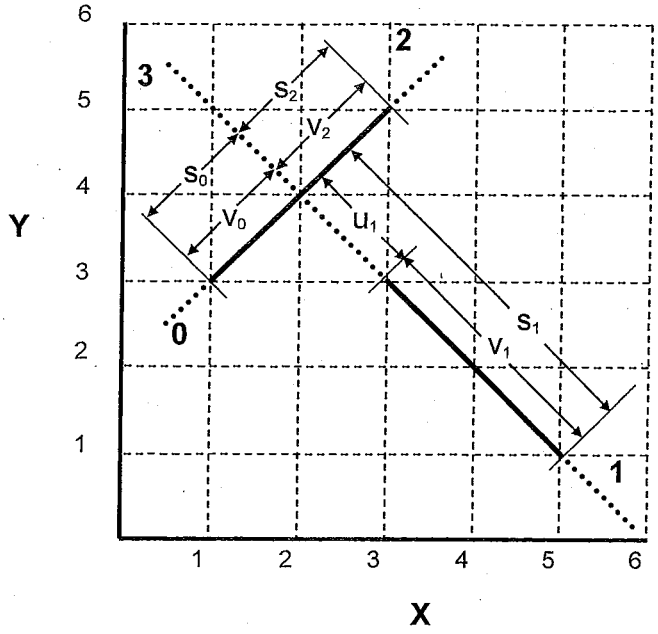

Figure 4. Specific case of two nonparallel line segments labeled for detailed computational analysis. Only segments of nonzero length are labeled.

shown in Figure 2a. Application of these configuration-specific formulas to other nonparallel configurations (Figure 2b–f) requires the use of the additional formulas discussed in Appendix B.

In the case of parallel line segments, such as those shown in Figure 3a, a standard derivation using integration is used, and its development is outlined in Appendix C. It is a straightforward, if somewhat tedious, derivation and therefore not presented in detail. Formulas for both the expected distance and the expected square of the distance are given. Any configuration where the extended lines of two segments are coincident, as illustrated in Figure 3b, must be handled separately. An examination of the limit as one line segment of Figure 3a approaches the extended parallel line of the second line segment provides the appropriately modified formula for segments lying on coincident lines.

All of these formulas for parallel and nonparallel line segments must be used in conjunction with computational formulas that extend their application to more general spatial configurations. Correctly implementing the computational side of these formulas is a critical second step because, even with the provision of convenient and comprehensive formulas, the chance of misinterpretation and subsequent programming error remains significant. Specific examples, two of which are tabulated here in detail, can be

Table 1. Individual segment labels and lengths for the four branches of the two intersecting lines illustrated in Figure 4

i	s_i	v_i	u_i
0	1.4142	1.4142	0.0000
1	4.2426	2.8284	1.4142
2	1.4142	1.4142	0.0000
3	0.0000	0.0000	0.0000

Table 2. Intermediate and final computational results for the four branches of the two intersecting lines shown in Figure 4

Δ*	λ_1	λ_2	λ_3	A^2	r_b	r_c	E_b	E_c	$F(\lambda_2, \lambda_3)$	$F(v_i, v_{i+1})$	Wt	$S(\lambda_2, \lambda_3)$	$S(v_i, v_{i+1})$
s_0s_1	4.4721	1.4142	4.2426	9.00	0.1623	0.7208	4.3199	2.6647	2.3282			6.6667	
u_0s_1	4.2426	0.0000	4.2426	0.00					0.0000			0.0000	
u_1s_0	2.0000	1.4142	1.4142	1.00	0.4142	0.4142	1.6232	1.6232	1.0822			1.3333	
u_0u_1	1.4142	0.0000	1.4142	0.00					0.0000			0.0000	
										2.9512	0.50		9.3333
s_1s_2	4.4721	4.2426	1.4142	9.00	0.7208	0.1623	2.6647	4.3199	2.3282			6.6667	
u_1s_2	2.0000	1.4142	1.4142	1.00	0.4142	0.4142	1.6232	1.6232	1.0822			1.3333	
u_2s_1	4.2426	0.0000	4.2426	0.00					0.0000			0.0000	
u_1u_2	1.4142	1.4142	0.0000	0.00					0.0000			0.0000	
										2.9512	0.50		9.3333
s_2s_3	1.4142	1.4142	0.0000	0.00					0.0000			0.0000	
u_2s_3	0.0000	0.0000	0.0000	0.00					0.0000			0.0000	
u_3s_2	1.4142	0.0000	1.4142	0.00					0.0000			0.0000	
u_2u_3	0.0000	0.0000	0.0000	0.00					0.0000			0.0000	
										0.0000	0.00		0.0000
s_3s_0	1.4142	0.0000	1.4142	0.00					0.0000			0.0000	
u_3s_0	1.4142	0.0000	1.4142	0.00					0.0000			0.0000	
u_0s_3	0.0000	0.0000	0.0000	0.00					0.0000			0.0000	
u_3u_0	0.0000	0.0000	0.0000	0.00					0.0000			0.0000	
										0.0000	0.00		0.0000
									$E\{D\} = F = 2.9512$			$E\{D^2\} = S = 9.3333$	

* The corresponding legs of the triangle branching from the intersection point.

used by future users to develop and confirm their own computational programs.

Figure 4 illustrates a case of two nonparallel line segments. One branch of the two intersecting lines is selected arbitrarily and the four branches are numbered sequentially, proceeding counterclockwise around the intersection point using the index variable i starting with zero. For each branch, $i = 0, 3$, we have $s_i = u_i + v_i$, where v_i is the length of that portion of the line segment falling on that particular branch and u_i is the distance from the intersection point to the nearest segment point on the branch. The branches for this example have been labeled as shown in the figure and the corresponding segment lengths calculated. These lengths are listed in Table 1. The aforementioned formulas and procedures yield the intermediate and final results presented in Table 2. Implementing the computational procedure requires that each pair of adjacent branches from the point of intersection of the two lines be evaluated. It will be noted in this example that branch pairs 2/3 and 3/0 do not contribute to the expected distance; they are included in Table 2, however, for the sake of procedural clarity for program developers.

The annotated case of two parallel line segments is shown in Figure 5. Segment lengths for this case are given in Table 3, and intermediate and final results based on the formulas and procedures provided in the appendixes are found in Table 4. The rational for providing formula derivations and these detailed computational results will become evident during the process of verification that follows.

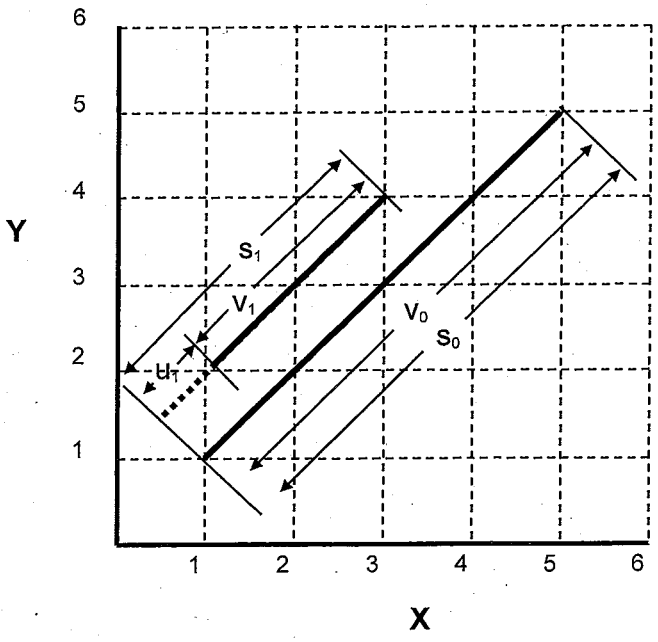

Figure 5. Specific case of two parallel line segments labeled for detailed computational analysis.

Verification

Lengthy formula and computer program developments increase the chance of analyst or programmer error. For this reason, it is of paramount importance to verify results. It is anticipated that the formulas and procedures of this article will be applied by others. That these users be able to verify their computer code is highly desirable. Examining computer output for conformity with independently developed

Table 3. Individual segment labels and lengths for the two parallel lines illustrated in Figure 5

i	s_i	v_i	u_i
0	5.6569	5.6569	0.0000
1	3.5355	2.8284	0.7071

Table 4. Intermediate and final computational results for the two parallel line segments shown in Figure 5

□*	λ_{12}	λ_{24}	λ_{13}	λ_{34}	λ_{14}	λ_{23}	Wt	$F(\lambda_{23}, \lambda_{14})$	Wt	$S(\lambda_{23}, \lambda_{14})$
s_0s_1	0.7071	3.6056	5.7009	2.2361	3.5355	5.6569	1.25	2.0092	1.25	5.3333
u_0s_1	0.7071	3.6056	0.7071	3.6056	3.5355	0.0000	0.00	0.0000	0.00	4.6667
u_1s_0	0.7071	1.0000	5.7009	5.0000	0.7071	5.6569	−0.25	2.6790	−0.25	9.3333
u_0u_1	0.7071	1.0000	0.7071	1.0000	0.7071	0.0000	0.00	0.0000	0.00	0.6667
								$F(v_0, v_1) = 1.8418$		$S(v_0, v_1) = 4.3333$

* The corresponding segment sides of the trapezoid.

results is an essential element of most verification processes. It is also advisable wherever possible to check for internal consistency of the formulas by examining values approached at limits or other special cases for which results have been independently established.

The crucial test of the formulas and computational procedures of this article consist of comparing their output with that of a numerical integration model (Appendix D). Each of the specific examples shown in Figures 1–3 was evaluated using the closed-form equations developed in this article as well as numerical integration. The comparative results for both the expected distance and the expected square of the distance were found to be in complete agreement with the number of decimal places listed in Tables 5 and 7 [3].

A comparison was then made with the results presented by Okabe and Miller (1996). All of their results, as calculated for pairs of perpendicular line segments, were in essential agreement with values calculated using the model of this article. There was, however, significant disagreement when comparing results for parallel line segments. To resolve this disagreement, further verification tests were run.

In one case, Okabe and Miller report an error of 12.3% for two parallel line segments. These two lines, taken from Figure 7 of their article, are appropriately scaled and graphed in Figure 6. Based on their reported error of 12.3%, the expected distance as calculated by their formula (not provided in their article) was determined to be 1.27. Using the closed-form equation developed in Appendix C of this article and the numerical integration procedure of Appendix D the expected distance in this instance was calculated to be 1.261 by both methods. Because of the small number of significant digits in the percentage error reported by Okabe and Miller, some caution must be exercised in the interpretation of these results. It is recommended at this time, however, that the formulas and procedures given here be preferentially used for the calculation of random distances between parallel lines. These comparative results strongly suggest that there is an ongoing need for meticulous verification of derived formulas as well as the results of their computational implementation. With this caveat in mind, another confirmatory test of the formulas and procedures of this article was run.

A cross verification of the formulas for parallel and nonparallel line segments was done using two variations of the example given in Figure 2a. In both variations, the first line segment was kept fixed as shown between points (2, 1) and (1, 5). In the first variation, one end point of the second line segment was kept at (2, 1) but the other end point was moved to (1.001, 5). These near-parallel lines gave an expected distance of 1.3743, and an expected square of the distance of 2.8332 when using the formulas for nonparallel lines. In the second variation, the second line segment was extended between points (2.001, 1) and (1.001, 5). In this variation, the parallel line formula was applied and yielded an expected distance of 1.3744 and an expected square of the distance of 2.8333. (These latter two values to four decimal places are also obtained if the second segment is made to exactly overlap the first.) The precise values for these two parameters for exactly superimposed segments

Table 5. Calculated population parameters for line segment configurations shown in Figures 2a–f and 3a, b

Figure	Population parameters		
	$E\{D\}$	$E\{D^2\}$	σ
2a	2.5212	7.1667	0.9001
2b	1.7568	3.6667	0.7618
2c	1.9776	4.3333	0.6499
2d	3.1074	9.8333	0.4211
2e	2.9512	9.3333	0.7898
2f	2.2409	5.8333	0.9009
3a	1.8418	4.3333	0.9701
3b	3.5355	13.3333	0.9129

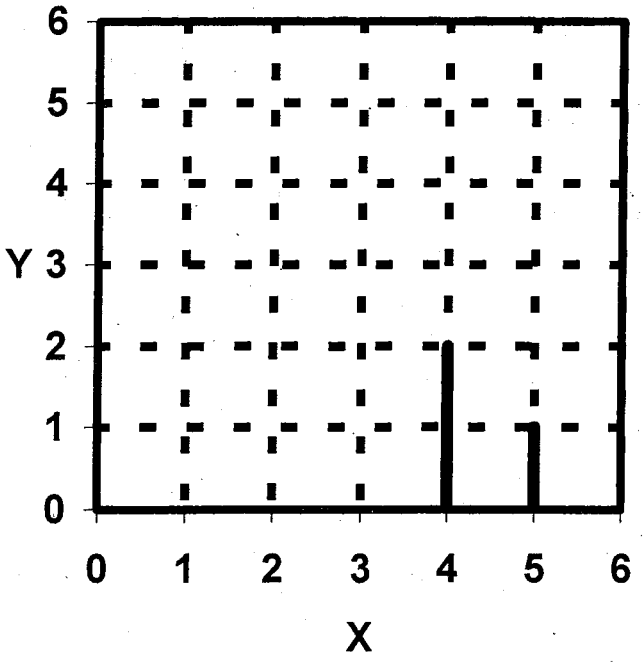

Figure 6. Scaled example taken for comparison from Okabe and Miller (1996).

are known to be given by $\lambda/3$ and $\lambda^2/6$, where λ is the length of the line segment (Conolly 1981). When applied to the line segment between (2, 1) and (1, 5), these formulas from Conolly yield values of 1.3744 and 2.8333, respectively. Although not conclusive evidence of correct formula development, these essentially equal values coming from separately derived equations lend an additional measure of support for the formulas of this article and their attendant programming implementation.

Illustrative Example Continued

For linked segments 1-2 and 3-4-5 of Figure 1, the probabilities that any one of a pair of concurrently burning ATIA fires will be observed somewhere along their two respective lengths are arbitrarily set, for purposes of illustration, at P{1-2} = 0.6 and P{3-4-5} = 0.4. It is assumed that the two random fire-start locations are distributed independently. Here also, for simplicity of presentation, it will be assumed that all follow-on fire-start locations to which the airtanker resource is assigned are statistically independent of current and previous fire-start locations and airtanker assignments [4]. Given that a fire occurs along linked segments 1-2, the probability that it is somewhere along segment 1 is given by the ratio of the length of segment 1 to the total length of both segments; i.e., P{1|1–2} = 6.3246/(6.3246 + 5.3852) = 0.5401. (This allocation of probability proportional to segment length is also an arbitrary, if convenient and sometimes logical, assumption.) Similar probabilities proportional to segment length are assigned to linked segments 3-4-5. For example, P{3|3-4-5} = 3.1623/(3.1623 + 3.1623 + 4.2426) = 0.2993. Based on probabilities derived in this manner, the ATIA transfer probabilities between line segments can be calculated (Table 6). Two examples should help clarify these calculations. The probability of airtanker transfer from a fire located somewhere on segment 3 to another fire also along segment 3 is calculated as the probability that the first fire is located on this segment; i.e., P{3-4-5} · P{3|3-4-5} = (0.4)(0.2993) = 0.1197, times the probability that the second fire is also on this segment (this second probability has the same value as the first), which gives the probability of this flight-distance event as 0.0143. As a second example, transfer from segment 3 to segment 1, or vice versa, has a combined probability given by P{3-4-5} · P{3|3-4-5} · P{1-2} · P{1|1-2} + P{1-2} · P{1|1-2} · P{3-4-5} · P{3|3-4-5}, which, on substituting the numerical probabilities, gives (0.4)(0.2993)(0.6)(0.5401) + (0.6)(0.5401)(0.4)(0.2993), yielding a value of 0.0776. It is to be acknowledged that all of these probabilities have been kept simple, and in practice, the nature and specification of fire occurrence probabilities merit careful research in their own right.

Table 6. Calculated transfer probabilities between line segments as illustrated in Figure 1

	1	2	3	4	5
1	0.1050	0.1788	0.0776	0.0776	0.1041
2	—	0.0761	0.0661	0.0661	0.0886
3	—	—	0.0143	0.0287	0.0384
4	—	—	—	0.0143	0.0384
5	—	—	—	—	0.0258

Table entry shown for line i to line j is also the probability of transfer from line j to line i.

The expected distance, the expected square of the distance, and the SD have been calculated for all possible transfer routings and are given in Table 7. When weighted by the probabilities of Table 6 the aggregated expectations of Table 8 are obtained.

The flight time between fires for this example application can now be easily found. The formula $T = D/V$ gives the flight time where V, the cruising speed, is assumed to be 250 km/hour. The expected time then is given by $E\{D\}/V$. Exercising some care with the units, this formula yields (42.2/250) = 0.169 hour (10.13 min.) as the mean flight time. The variance of the flight time is given by $\text{var}\{D\}/V^2$. This formula can be written as $[E\{D^2\} - E\{D\}^2]/V^2$. Once again using some care with the units, the formula yields $[2{,}264 - 42.2^2]/250^2 = 0.00773$. A SD expressed in minutes is more intuitively appealing and a value of 5.27 min is obtained for this parameter. These are the operational parameters sought for airtanker planning in this particular example. Although the example is quite simple, it has captured most of the essential elements of the proposed analytical description of airtanker redirection in a fully reproducible way.

Concluding Observations

Substantial work remains before these promising analytical results might be considered ready for practical application in the modeling of airtanker resource allocation decisions. Remaining work includes the analytical evaluation of flight-distance moments from lines to areas as well as between areas, the analytic determination of third and possibly higher moments of the flight-distance distribution, and

Table 7. Computed population parameters for the one-way transfer distance between the line segments of Figure 1

	1	2	3	4	5
$E\{D\}$					
1	2.1082	5.4152	5.4563	4.0399	6.2260
2	—	1.7951	6.7940	4.7462	3.0657
3	—	—	1.0541	2.4198	5.2262
4	—	—	—	1.0541	3.6231
5	—	—	—	—	1.4142
$E\{D^2\}$					
1	6.6667	34.0000	30.6667	16.6667	41.3333
2	—	4.8333	46.5000	23.5000	10.1667
3	—	—	1.6667	6.6667	28.3333
4	—	—	—	1.6667	15.3333
5	—	—	—	—	3.0000
σ					
1	1.4907	2.1623	0.9460	0.5884	1.6031
2	—	1.2693	0.5847	0.9868	0.8766
3	—	—	0.7454	0.9008	1.0102
4	—	—	—	0.7454	1.4855
5	—	—	—	—	1.0000

Table 8. Aggregate population parameters for the protection components shown in Figure 1

$E\{D\}$	$E\{D^2\}$	σ
4.2216	22.6436	2.1958

the evaluation of near-parallel lines that exhibit ill conditioning in the calculation of their intercept point.

Okabe and Miller (1996) give formulas for random distances from lines to areas and from areas to areas. Confirmation of these formulas and extension of their range of application should be carried out. Of particular interest in this latter regard is the analytical evaluation of the flight distance between two random points within a single area. Computational procedures based on the derived formulas must also be developed and verified.

There is some indication that airtanker cost functions are nonlinear in flight distance within their range of application (Dobson 1965). If it is desirable to statistically evaluate these cost functions when they are expressed as power series, then higher moments of travel distance will have to be developed (Ang and Tang 1975). If only for descriptive purposes, the availability of the third moment would be of value in the identification and summary characterization of those flight-distance distributions that are strongly skewed.

In the evaluation of two nonparallel line segments, the point of intersection of their extended lines must be calculated. For lines that are very nearly but not quite parallel, this ill conditioning can potentially lead to significant computational error. In a related issue, it is noted that, as two nonparallel line segments approach parallelism, there is a point at which a more accurate answer for the expected flight distance will be given by the formula for parallel lines. The practical importance of these issues in application should be examined and procedures developed to address them if found to be warranted.

In their development of an initial attack queuing model, Islam and Martell (1998) list several elements composing ATIA service time. The elements mentioned are mobilization time, flight time from the airbase to the fire and back, and firefighting time. To achieve a more accurate description of ATIA system behavior, especially during periods of high daily fire loads, it is proposed that the definition of service time include a time element for airtanker reallocation between fires. It has been the purpose of this article to initiate an examination of this reallocation element by developing an analytical procedure for calculating the flight distance between randomly located fires on line segments. First and second moments of the random flight-distance variable, analytically developed and providing exact values for line segments, are now available in a comprehensive computational format. The actual incorporation of these results in an initial attack model awaits further research developments, including those here mentioned, but these results do represent a solid first step toward statistical specification of fire-to-fire airtanker transfer distances.

Endnotes

[1] This assumption may be questionable in practice where it seems quite likely that flight speed may be found to have both significant variability and positive correlation with distance.

[2] The use of a homogeneous Poisson process leading to a uniform distribution of service points is a generally accepted assumption in the development of models of this type (Larson and Odoni 1981). Here, for purposes of model development and illustration, it is assumed that airtanker initial-attack fires are, likewise, identically and independently distributed. The application and concurrent validation of this model with respect to a documented real-world example is a separate topic, well beyond the purpose and scope of this article.

[3] The results reported here were also independently confirmed using Monte Carlo simulation. These simulation results are not reported in this article due to considerations of length and the primacy of verification through numerical integration.

[4] In this context, it is noted that the assumption of independently distributed fire-start locations may be a questionable assumption for some fire protection regions, especially where arson- or lightning-caused fires are frequently observed (Greulich 2003). The identification and statistical description of such spatial–temporal clustering is an area of active research by others and is well beyond the scope and purpose of this article.

[5] The reader will note that Monte Carlo simulation is easily executed using these formulas by generating two random points (x, y) and (u, v) for the distance formula using values of τ_1 and τ_2 distributed uniformly over the interval [0; 1].

Literature Cited

ANG, A.H-S., AND W.H. TANG. 1975. Probability concepts in engineering planning and design, vol. I: Basic principles. John Wiley and Sons, New York. 409 p.

CONOLLY, B. 1981. Techniques in operational research, vol. 2: Models, search and randomization. John Wiley and Sons, New York 340 p.

DOBSON, N.R. 1965. The economics of the Canadair CL-215 in the waterbomber and passenger transport roles. Canadair Ltd., Montreal, Quebec, Canada. OER-452.

GASKELL, R.E. 1958. Engineering mathematics. Holt, Rinehart and Winston, Inc. New York. 462 p.

GREULICH, F.E. 2003. Airtanker initial attack: A spreadsheet-based modeling procedure. Can. J. For. Res. 33(2):232–242.

ISLAM, K.M.S., AND D.L. MARTELL. 1998. Performance of initial attack airtanker systems with interacting bases and variable initial attack ranges. Can. J. For. Res. 28(10):1448–1455.

KENDALL, M.G., AND P.A.P. MORAN. 1963. Geometrical probability. Hafner Publishing Company, New York. 125 p.

LARSON, R.C., AND A.R. ODONI. 1981. Urban operations research. Prentice-Hall, Inc., Englewood Cliffs, NJ. 573 p.

MARTELL, D.L., A. TITHECOTT, AND P.C. WARD. 1999. Fighting fire with OR. OR/MS Today. 26(2):48–51.

OKABE, A., AND H.J. MILLER. 1996. Exact computational methods for calculating distances between objects in a cartographic database. Cartog. and Geog. Infor. Sys. 23(4):180–195.

SMITH, E.L. 1987. A fire management simulation model using stochastic arrival times. USDA For. Serv. Res. Pap. PSW-189.

Appendix A

The following derivation of the mean distance between randomly selected points on two separate straight-line segments uses Crofton's theorem on fixed points (Kendall and

Moran 1963). Larson and Odoni (1981) offer an excellent introduction to the use of Crofton's methodology that is most relevant to the development that follows. In this particular development, a previously derived formula for the expected distance from a fixed point to a random point on any line segment is used (Greulich 2003). The resulting differential equation is solved for the desired result. A formula is also given, without derivation, for the second moment about the origin.

With reference to Figure 7 the expected distance from the straight-line segment *ab* to segment *ac* is denoted M(y) and the expected distance from segment *ab'* to segment *ac'* is denoted M($y + \Delta y$). It is observed that the Cartesian coordinates of a point uniformly distributed along the line segment *ab'* have a y-coordinate that is uniformly distributed between 0 and $y + \Delta y$. A similar observation applies to a uniformly distributed point along the segment *ac'*. Hence it is possible to write, for example, that

Prob{Random Point falls on *cc'*}

$$= \frac{\text{length } cc'}{\text{length } ac'} = \frac{\Delta y}{y + \Delta y}, \tag{A1}$$

with similar expressions for the probability that a randomly selected point falls on segments *bb'*, *ac*, and *ab*. Using these probabilities, it is possible to condition on the corresponding four partitions of the two line segments, obtaining as a result

$$\mathrm{M}(y + \Delta y) = \left(\frac{y}{y + \Delta y}\right)^2 \mathrm{M}(y) + \left(\frac{y\Delta y}{(y + \Delta y)^2}\right)\mathrm{E}_b + \left(\frac{y\Delta y}{(y + \Delta y)^2}\right)\mathrm{E}_c + \left(\frac{\Delta y}{(y + \Delta y)}\right)^2 \mathrm{W}, \tag{A2}$$

where the following variables are defined: E_b is the expected distance from a point falling between *b* and *b'* to the line segment *ac*, E_c is the expected distance from a point between *c* and *c'* to the line segment *ab*, and W is the expected distance between a point on *bb'* and a point on *cc'*.

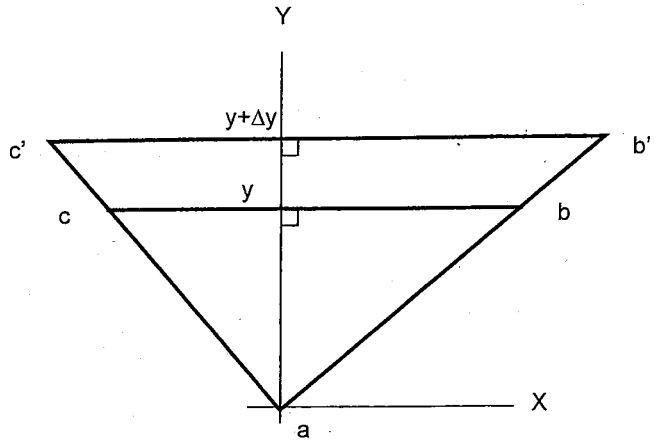

Figure 7. Two line segments *ab* and *ac* forming the legs of a triangle that has been oriented and extended for analysis.

Simplify Equation A2 and form the finite difference relationship

$$\frac{\mathrm{M}(y + \Delta y) - \mathrm{M}(y)}{\Delta y} = \frac{y(\mathrm{E}_b + \mathrm{E}_c) + \mathrm{W}\Delta y - 2y\mathrm{M}(y) - \mathrm{M}(y)\Delta y}{y^2 + 2y\Delta y + \Delta y^2}, \tag{A3}$$

which, on letting Δy go to zero and simplifying, yields

$$\frac{\mathrm{dM}(y)}{\mathrm{d}y} = \frac{\mathrm{E}_b + \mathrm{E}_c - 2\mathrm{M}(y)}{y}, \tag{A4}$$

which is the desired differential equation consistent with Crofton's formula. Formulas for the expected distances E_b and E_c must now be inserted.

A formula for the expected distance from a fixed point to a randomly selected point on a line segment has been given elsewhere (Greulich 2003). A minor modification of this formula will facilitate subsequent development of the above differential equation. By applying basic trigonometric relationships to the triangle of either Figure 8a or 8b, the following formulas, equally applicable to both cases, are easily derived for the indicated side lengths:

$$\lambda_1 = y\left(\frac{\cos\Theta_2}{\sin\Theta_2} + \frac{\cos\Theta_3}{\sin\Theta_3}\right) \tag{A5a}$$

$$\lambda_2 = y\left(\frac{1}{\sin\Theta_3}\right) \tag{A5b}$$

$$\lambda_3 = y\left(\frac{1}{\sin\Theta_2}\right) \tag{A5c}$$

In these equations, it is observed that the lengths of the triangle sides are proportional to the value of y and that, for any change in the triangle height, y, the angles Θ_i, which are parameters defining the shape of the triangle, remain fixed. It is likewise easily found that the area, A, of the triangle is given by

$$A = \left(\frac{y^2}{2}\right)\left(\frac{\cos\Theta_2}{\sin\Theta_2} + \frac{\cos\Theta_3}{\sin\Theta_3}\right). \tag{A5d}$$

Here the area is observed to be proportional to the square of y. With these results in hand, the expected distance from a point to a random location on a line segment is examined.

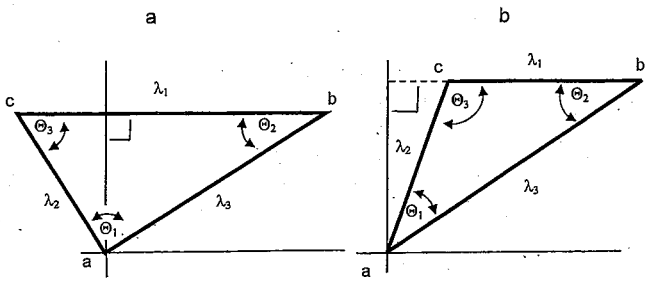

Figure 8. The two possible triangular configurations oriented for analysis with side and angle labeling.

Applying the previously mentioned formula for the expected distance the following equations are obtained:

$$E_b = \left[\frac{\lambda_1 + \lambda_3}{4}\right]\left[1 + \left(\frac{\lambda_1 - \lambda_3}{\lambda_2}\right)^2\right] + \left[\frac{2A^2}{\lambda_2^3}\right]\left[\ln\left(\frac{1 + r_b}{1 - r_b}\right)\right] \tag{A6a}$$

and

$$E_c = \left[\frac{\lambda_1 + \lambda_2}{4}\right]\left[1 + \left(\frac{\lambda_1 - \lambda_2}{\lambda_3}\right)^2\right] + \left[\frac{2A^2}{\lambda_3^3}\right]\left[\ln\left(\frac{1 + r_c}{1 - r_c}\right)\right], \tag{A6b}$$

where

$$r_b \equiv \frac{\lambda_2}{\lambda_1 + \lambda_3} \tag{A7a}$$

and

$$r_c \equiv \frac{\lambda_3}{\lambda_1 + \lambda_2} \tag{A7b}$$

and, in terms of the λ_i,

$$A = \left\{\frac{-[\lambda_3^2 - (\lambda_1 - \lambda_2)^2][\lambda_3^2 - (\lambda_1 + \lambda_2)^2]}{16}\right\}^{1/2}. \tag{A8}$$

By substitution of Equations A5a–d, the equation for E_b could, if desired, be written in terms of the variable y and the Θ_i parameter values. The following equation abbreviates this substitution process:

$$E_b = yK_b, \tag{A9a}$$

where K_b is a function only of the Θ_i values and is invariant for any particular triangle of interest. The formula for E_c may be written in a similar fashion,

$$E_c = yK_c. \tag{A9b}$$

Substitute Equations A9a and b into Equation A4, simplify, and define $K \equiv\equiv K_b + K_c$ to obtain

$$\frac{dM(y)}{dy} = K - \frac{2M(y)}{y}. \tag{A10}$$

Equation A10 is a linear differential equation of the first order that is readily solved (Gaskell 1958), giving the solution

$$M(y) = \frac{Ky}{3} = \frac{E_b + E_c}{3}, \tag{A11}$$

which can be most conveniently solved for a numerical solution using Equations A6a–A8. This formula for the first moment of the random distance variable between line segments λ_2 and λ_3 will be denoted as $F(\lambda_2, \lambda_3)$. This is an abbreviated notation for the equation because λ_1 is not listed but is understood to be present.

A similar development provides a formula for the second moment about the origin (also written in abbreviated form),

$$S(\lambda_2, \lambda_3) = \left[\frac{6\lambda_1^2 + 2\lambda_2^2 + 2\lambda_3^2}{24}\right]. \tag{A12}$$

Appendix B

In this appendix, a formula is developed for the weighted mean distance between any two nonparallel line segments. This formula accommodates line segments that either cross the point of intersection of their extended lines or not. There are six possible configurations, and examples of these are illustrated in Figure 2. The expected distance formula of Appendix A, as presented, is immediately applicable only to line segments configured as shown in Figure 2a. The weighting process developed in this appendix extends the use of this formula to cover all conceivable nonparallel cases. (In fact, the same final weighting formula derived here is equally applicable to the case of parallel line segments as configured and discussed in Appendix C.)

Figure 9 is an enlarged and further annotated representation of the configuration shown in Figure 2d. This configuration will serve to illustrate the development of the weighting formula. One branch of the intersecting lines is selected arbitrarily, and the branches are numbered sequentially for subsequent indexing using the variable i. Branch indexing starts with zero and proceeds counterclockwise. For each branch i ($i = 0, 3$) we have $s_i = u_i + v_i$, where v_i is the length of that portion of the line segment falling on that particular branch, and u_i is the distance from the intersection point to the nearest segment point on the branch. It is noted that u_i and v_i can be zero on some of the branches, as is observed here where u_2, v_2, u_3, and v_3 are all zero.

The mean distance for the length of a line connecting randomly selected points on segments u_i and u_{i+1} is denoted $F(u_i, u_{i+1})$, the first moment about the origin for the distribution. In a similar fashion and more specifically for this configuration, it is possible to write

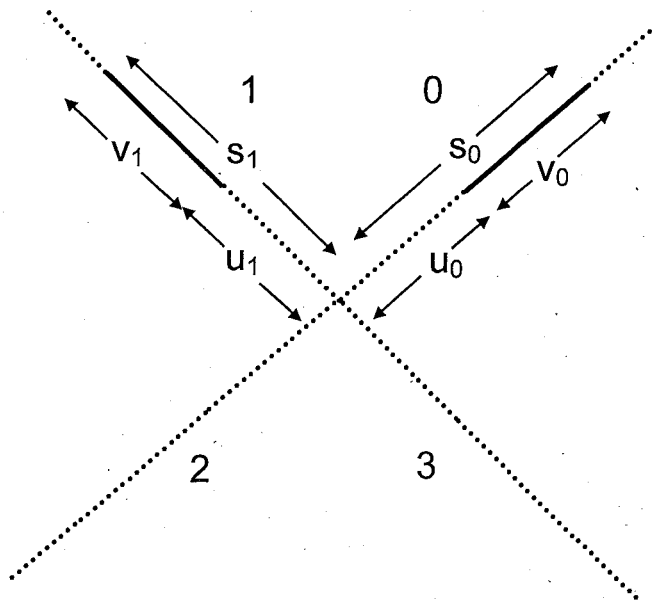

Figure 9. Labeling of intersecting line components for analysis of a more general case.

$$F(u_0, s_1) = \left[\frac{u_1}{s_1}\right]F(u_0, u_1) + \left[\frac{v_1}{s_1}\right]F(u_0, v_1). \quad \text{(B1)}$$

Minor manipulation of this formula gives

$$F(u_0, v_1) = \left[\frac{s_1}{v_1}\right]F(u_0, s_1) - \left[\frac{u_1}{v_1}\right]F(u_0, u_1). \quad \text{(B2)}$$

Starting with a similar formula for $F(u_1, s_0)$ it is found that

$$F(u_1, v_0) = \left[\frac{s_0}{v_0}\right]F(u_1, s_0) - \left[\frac{u_0}{v_0}\right]F(u_1, u_0). \quad \text{(B3)}$$

It is also possible to write

$$F(s_0, s_1) = \left[\frac{u_0}{s_0}\frac{u_1}{s_1}\right]F(u_0, u_1) + \left[\frac{u_0}{s_0}\frac{v_1}{s_1}\right]F(u_0, v_1) + \left[\frac{v_0}{s_0}\frac{u_1}{s_1}\right]F(v_0, u_1) + \left[\frac{v_0}{s_0}\frac{v_1}{s_1}\right]F(v_0, v_1). \quad \text{(B4)}$$

Substitute B2 and B3 into B4 and simplify to

$$F(v_0, v_1) = \left[\frac{1}{v_0 v_1}\right][(s_0 s_1)F(s_0, s_1) - (u_0 s_1)F(u_0, s_1) - (u_1 s_0)F(u_1, s_0) + (u_0 u_1)F(u_0, u_1)]. \quad \text{(B5)}$$

The significance of this final equation is that the formula derived in Appendix A can now be applied to all of the expected distance terms on the right-hand side of the equation yielding the sought-after expected distance between the two line segments v_0 and v_1. This equation can be immediately modified for calculation of the second moment, $S(v_0, v_1)$.

A final, general weighting process is needed to calculate the expected distance. This formula is equally applicable to any of the configurations illustrated in Figure 2. To arrive at this weighting formula, the possible contribution to the mean distance from each adjacent pair of the four branches must be aggregated. The use of modulo 4 indexing provides a convenient shorthand. This indexing process can be illustrated using the fact that the following probabilities must sum to one:

$$\sum_{\substack{i=0 \\ \text{Mod } 4}}^{3} \left[\frac{v_i}{v_i + v_{i+2}}\right]\left[\frac{v_{i+1}}{v_{i+1} + v_{i+3}}\right] = 1.0, \quad \text{(B6)}$$

that is,

$$\left[\frac{v_0}{v_0 + v_2}\right]\left[\frac{v_1}{v_1 + v_3}\right] + \left[\frac{v_1}{v_1 + v_3}\right]\left[\frac{v_2}{v_2 + v_0}\right] + \left[\frac{v_2}{v_2 + v_0}\right]\left[\frac{v_3}{v_3 + v_1}\right] + \left[\frac{v_3}{v_3 + v_1}\right]\left[\frac{v_0}{v_0 + v_2}\right] = 1.0. \quad \text{(B7)}$$

Finally then, the weighted mean distance from a randomly located point on one line segment to a randomly located point on another line segment is calculated, in general, by

$$F = \sum_{\substack{i=0 \\ \text{Mod } 4}}^{3} \left(\frac{v_i}{v_i + v_{i+2}}\right)\left(\frac{v_{i+1}}{v_{i+1} + v_{i+3}}\right)F(v_i, v_{i+1}) \quad \text{(B8)}$$

and the second moment by

$$S = \sum_{\substack{i=0 \\ \text{Mod } 4}}^{3} \left(\frac{v_i}{v_i + v_{i+2}}\right)\left(\frac{v_{i+1}}{v_{i+1} + v_{i+3}}\right)S(v_i, v_{i+1}) \quad \text{(B9)}$$

Appendix C

A formula for the expected straight-line distance between parallel lines has also been derived. This derivation follows a more traditional approach, which will not be shown in detail. Attention is limited to only the general development techniques that lead directly to the several results needed for computational purposes.

The somewhat tedious derivation of the formula can be abbreviated by the following approach. Two parallel lines are constructed as shown in Figure 10. The integration will be carried out over segment λ_{23}. At any point y on this segment, the expected distance to segment λ_{14} can be separated into two parts, each of which is a right triangle. The expected distance formula for a right triangle may be readily developed. By way of example with reference to the illustrated side lengths of triangle 1, the appropriate formula would be

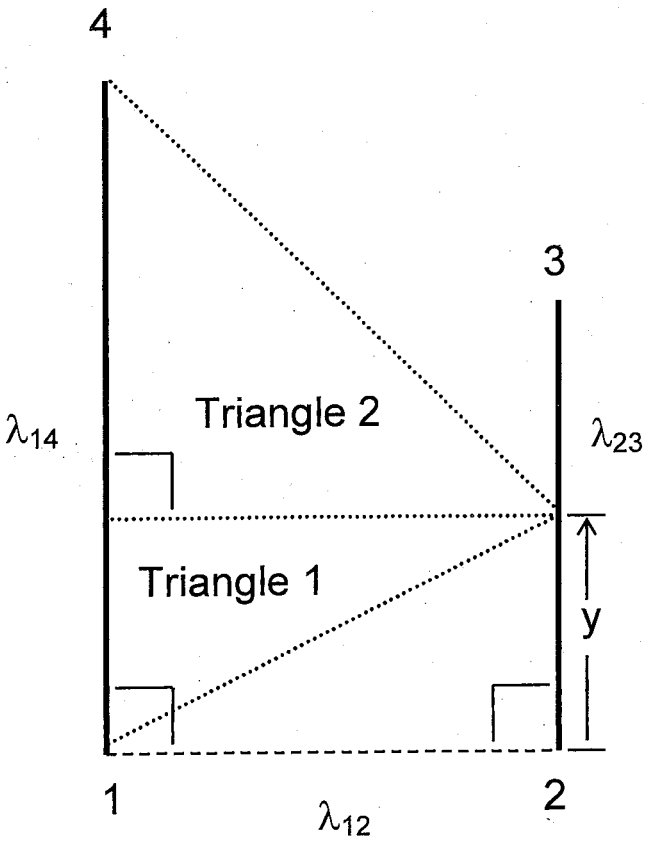

Figure 10. Two line segments forming the parallel sides of a trapezium oriented for analysis.

Avg Dist for Triangle 1

$$= \left[\frac{(y^2 + \lambda_{12}^2)^{1/2}}{2}\right] + \left[\frac{\lambda_{12}^2}{2y}\right]\log_e\left\{\frac{(y^2 + \lambda_{12}^2)^{1/2} + y}{\lambda_{12}}\right\}. \quad \text{(C1)}$$

This formula, together with a similar formula for triangle 2 when weighted by (y/λ_{14}) and $(\lambda_{14} - y)/\lambda_{14}$, respectively, and integrated over segment λ_{23} yields the following result for the expected distance:

$$F(\lambda_{23}, \lambda_{14}) = \left\{\frac{1}{2\lambda_{14}\lambda_{23}}\right\}\left\{\left[\frac{1}{3}\right][\lambda_{13}^3 - \lambda_{34}^3 - \lambda_{12}^3 + \lambda_{24}^3] \cdot \right.$$
$$\left. + [\lambda_{12}^2][-\lambda_{13} + \lambda_{34} + \lambda_{12} - \lambda_{24}]\right\}$$
$$+ \left\{\frac{\lambda_{12}^2}{2\lambda_{14}\lambda_{23}}\right\}\left\{\left[\lambda_{14}\log_e\left(\frac{\lambda_{14} + \lambda_{24}}{\lambda_{14} - \lambda_{23} + \lambda_{34}}\right)\right]\right.$$
$$\left. + \left[\lambda_{23}\log_e\left(\frac{\lambda_{23} + \lambda_{13}}{\lambda_{23} - \lambda_{14} + \lambda_{34}}\right)\right]\right\}. \quad \text{(C2)}$$

The lengths λ_{ij} are defined as shown in Figure 11. It is observed with respect to this formula that interchanging the two initial line segments (λ_{23} and λ_{14}), the shorter with the longer, does not change equation results.

Under certain conditions when the two line segments fall on the same extended line, there will be a division by zero error. To avoid this difficulty, the following formula, which is found as the general limit when λ_{12} goes to zero, should be applied:

$$F(\lambda_{23}, \lambda_{14}) = \left\{\frac{1}{2\lambda_{14}\lambda_{23}}\right\}\left\{\left[\frac{\lambda_{13}^3 - \lambda_{34}^3 + \lambda_{24}^3}{3}\right]\right\}. \quad \text{(C3)}$$

The expected square of the random distance from one line segment to the other is less tedious in its derivation and is given by the formula

$$S(\lambda_{23}, \lambda_{14}) = [1/6][6\lambda_{12}^2 + 2\lambda_{14}^2 - 3\lambda_{14}\lambda_{23} + 2\lambda_{23}^2]. \quad \text{(C4)}$$

To apply Equations C2–C4 to the general case of parallel line segments, a weighting procedure is required. With reference to line lengths as defined in Figure 12, the appropriate weighted value for the mean distance is once again given by Equation B5. The same weights are applied in calculating the weighted expected square of the random distance. Two examples of situations involving parallel lines are shown in Figure 3.

Appendix D

Numerical integration represents an alternative to the procedures developed and presented in this article. It is an alternative, however, that comes with the comparative disadvantage of higher computational cost for a result that is only an approximation to the exact value. In contrast, the new procedures given in this article provide exact results with modest computational effort. Numerical integration does, however, provide an expedient means of verifying the specific results given by these new procedures. Numerical

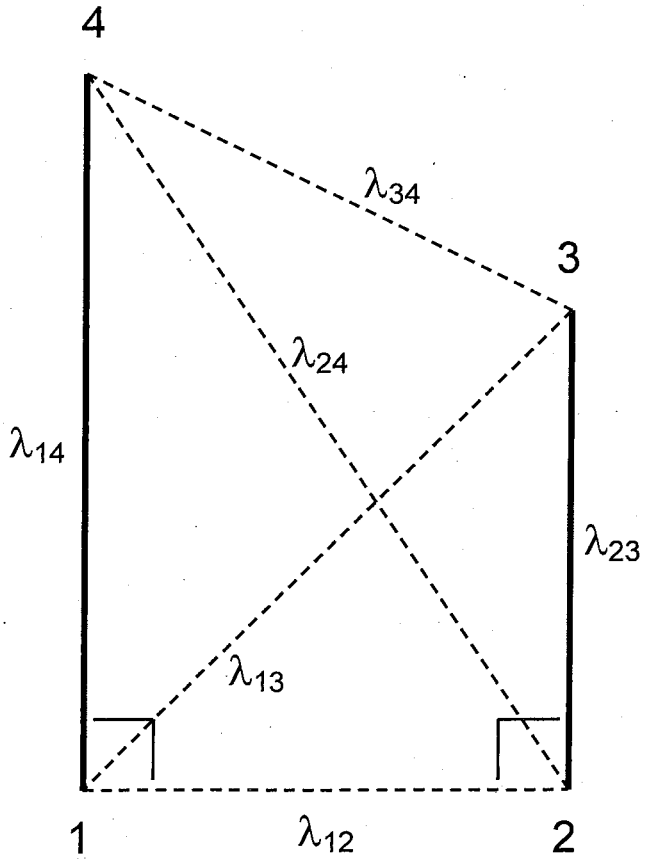

Figure 11. Detailed labeling of lengths for trapezium evaluation.

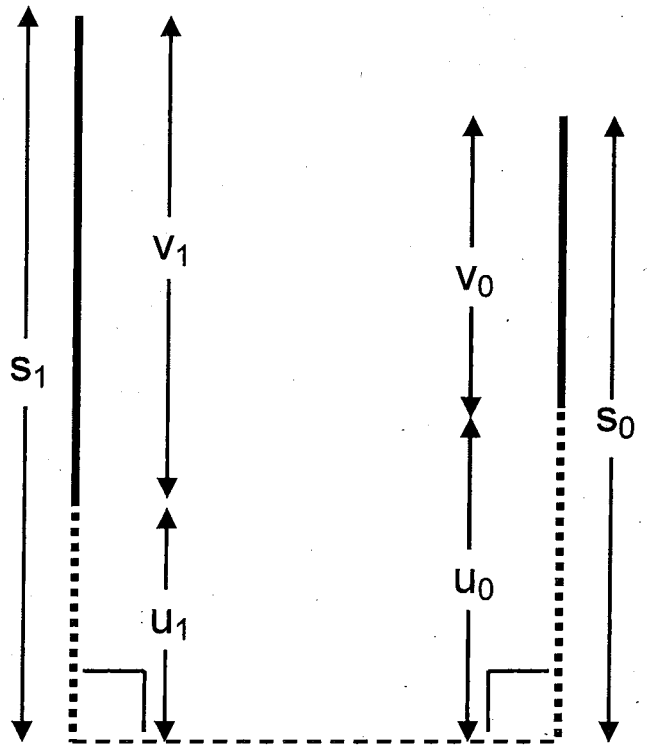

Figure 12. Labeling of parallel line components for analysis of a more general case.

integration for statistical parameters in the current case of random distances between two line segments can be executed as follows.

A point is to be randomly located on a line segment extending from (x_1, y_1) to (x_2, y_2). Let τ_1 be a random variable uniformly distributed over the interval [0, 1]. The coordinates of the random point (x, y) along the line segment may be written in parametric form as $[x_1 + \tau_1(x_2 - x_1), (y_1 + \tau_1(y_2 - y_1)]$. A second, independently distributed, random point is to be located along a line from (u_1, v_1) to (u_2, v_2). A similar parametric equation, here using τ_2 as an independent and uniformly distributed random variable over [0, 1], may be written for the random point (u, v) on this second line segment. The distance from the point on the first line segment to the point on the second can now be written as a function of τ_1 and τ_2 simply by substituting for (x, y) and (u, v) in the distance formula $D = [(x - u)^2 + (y - v)^2]^{1/2}$. Because the beginning and ending points of the line between the two segments are random variables, the length of this line, the flight distance, is also a random variable and its expected value may be written as

$$E\{D\} = \int_0^1 \int_0^1 D(\tau_1, \tau_2)\, d\tau_1\, d\tau_2, \qquad (D1)$$

and the expected square of the distance as

$$E\{D^2\} = \int_0^1 \int_0^1 [D(\tau_1, \tau_2)]^2\, d\tau_1\, d\tau_2, \qquad (D2)$$

These two formulas can be numerically approximated by

$$E\{D\} \approx \sum_{i=1}^{n} \left[\sum_{j=1}^{m} D(\tau_{1,j}, \tau_{2,i}) \Delta\tau_1 \right] \Delta\tau_2 \qquad (D3)$$

and

$$E\{D^2\} \approx \sum_{i=1}^{n} \left[\sum_{j=1}^{m} [D(\tau_{1,j}, \tau_{2,i})]^2 \Delta\tau_1 \right] \Delta\tau_2, \qquad (D4)$$

where $\tau_{1,j} = (1/m)(j - \frac{1}{2})$ and $\tau_{2,i} = (1/n)(i - \frac{1}{2})$ with finite differences $\Delta\tau_1 = 1/m$ and $\Delta\tau_2 = 1/n$. The number of subdivisions, m and n, of the line segments are analyst-specified such that they provide requisite accuracy in the approximation [5].